Research paper J. Electrochem. Sci. Technol. 5(4), 109-114 (2014)

Journal of Electrochemical Science and Technology

The Electrochemical Performance of $Li_3V_2(PO_4)_3$/Graphene Nano-powder Composites as Cathode Material for Li-ion Batteries

Mansoo Choi[1,2], Hyun-Soo Kim[1], Young Moo Lee[2], and Bong-Soo Jin[1]*

[1]*Battery Research Center, Korea Electrotechnology Research Institute, Changwon 642-120 Korea*

[2]*Dept. of Energy Engineering, Hanyang University, Seoul 133-791 Korea*

ABSTRACT

The $Li_3V_2(PO_4)_3$/graphene nano-particles composite was successfully synthesized by a facile sol-gel method. The addition of a graphene in $Li_3V_2(PO_4)_3$(LVP) showed the high crystallinity and influenced the morphology of the $Li_3V_2(PO_4)_3$ particles observed in X-ray diffraction (XRD) and scanning electron microscopy (SEM). The LVP/graphene samples were well connected, resulting in fast charge transfer. The effect of the addition graphene nano-particles on electrochemical performance of the materials was investigated. Compared with the pristine LVP, the LVP/graphene composite delivered a higher discharge capacity of 122 mAh g^{-1} at 0.1 C-rate, better rate capability and cyclability in the potential range of 3.0-4.3 V. The electrochemical impedance spectra (EIS) measurement showed the improved electronic conductivity for the LVP/graphene composite, which can ensure the high specific capacity and rate capability.

Keywords: Lithium vanadium phosphate, graphene nano-powder, electrical conductivity, Li-ion battery.

Received January 30, 2014 : Revised February 3, 2014 : Accepted March 6, 2014

1. Introduction

The Li-ion batteries (LIBs) have been regarded as one of the promising source to satisfy the growing demand of energy storage system, because the LIBs have numerous advantages of the high capacity, high operating voltage and long cycle life [1-3]. As the properties of the cathode material determine the performance of the LIB, it is essential to develop the new active materials for the cathode in advanced battery systems. Recently, the monoclinic $Li_3V_2(PO_4)_3$ has been considered as cathode materials for the advanced LIBs due to the lithium ion mobility, high reversible capacity, high operating voltage and safety [4-9]. It can also reversibly extract/insert two lithium ions between 3.0 and 4.3 V based on the V^{3+}/ V^{4+} redox couple (1 C = 133 mAh g^{-1}). However, despite of these advantages, the intrinsic low electronic conductivity of about 2.3×10^{-8} Scm^{-1} at room temperature, which is major drawback for the application of the LIBs, limits its rate capability [6,10]. In order to improve the low electronic conductivity, many efforts such as minimizing the particle size, doping with metal or surface coating with conducting materials were conducted [11-22]. Although the carbon coating is generally employed as a useful method towards improving the electronic conductivity of the LVP, it is difficult to cover uniformly the carbon on the surface

*Corresponding author. Tel.: 010-9412-2724

E-mail address: teracms@naver.com

Open Access DOI: http://dx.doi.org/10.5229/JECST.2014.5.4.109

of the LVP particles. The inhomogeneous surface coating results in decreasing the charging-discharging capacity at higher current rates because of the lack of the conducting network. The uniform carbon coating is important factor for the high discharge capacity, long cyclability, especially at high current rate. Recently, the graphene which is a single sheet of carbon atoms packed in a hexagonal lattice has emerged due to the outstanding electrical conductivity, ultra high surface area, good mechanical strength and chemical stability. The LVP/graphene composites were reported as cathode materials for LIBs [22]. They have suggested the effects of the graphene such as improved electronic conductivity, high surface area, effective carbon coating and nanoparticle size of the LVP particles. Although the LVP/graphene composite reported the positive effects, it required multi-steps for sample preparation and was not suitable for large scale.

In this study, we have synthesized the LVP/graphene composite through the facile sol-gel method by adding graphene nano-particles and investigated the structure and electrochemical performances. The addition of graphene nano-particles showed the high crystallinity and fine LVPparticles, which prevented the particle growth of the LVP. The effects of the graphene on the electrochemical performances resulted in the increased discharge capacity, good rate capability and cyclability of the cathode materials for the LIBs.

2. Experimental

For the synthesis of LVP composites, V_2O_5, $C_2H_2O_4{\cdot}H_2O$, $NH_4H_2PO_4$ and Li_2CO_3 were used as starting materials. The LVP particles were synthesized by using a sol-gel method reported in Ref. [22]. Briefly, V_2O_5 and oxalic acid were dissolved in a deionized water (DI) in a stoichiometric ration 1:3 and stirred at 80°C until clear blue solution was obtained (Eq. 1). Thereafter, $NH_4H_2PO_4$ and Li_2CO_3 were added to the solution and stirring for 5 h to evaporate the water. The gel-formed solution was dried at 100°C in an air overnight. The dried precursor was grounded and decomposed at 350°C for 4h and 800°C for 8h under an Ar atmosphere (Eq. 2).

$$V_2O_5 + 3H_2C_2O_4 \rightarrow 2VOC_2O_4 + 2CO_2 + 3H_2O \quad (1)$$

$$4VOC_2O_4 + 3Li_2CO_3 + 6NH_4H_2PO_4 \rightarrow 2Li_3V_2(PO_4)_3 + 9CO_2 + 2CO + 6NH_3 + 9H_2O \quad (2)$$

For the LVP/graphene composite, the desired amount of graphene nano-powder (ER-4400 graphene, IDT international) was put into the DI water and ultrasonicated for 1hr. The graphene powder was synthesized by modified Hummers method. The surface area and thickness of graphene was 200-250 m^2/g and below 5 nm, respectively. 5 g of LVP precursor was added into the graphene solution and followed by ultrasonic treatment for 1h. The LVP/graphene solution was kept for 20hr and then the temperature was increased to 80°C until LVP/graphene-gel was formed. After that, the LVP/graphene-gel was prepared in the same way of LVP preparation method.

The morphology of the samples was investigated by a field emission scanning electron microscopy (FE-SEM) working at 30kV. The power X-ray diffraction patterns of composites were conducted between 10° and 80° at a scan rate of 0.02° 2θ/min. Raman measurement was conducted with a laser wavelength of 532 nm.

The LVP/graphene composite electrode was prepared by mixing active material, Super P, and PVDF in a wt. ratio of 70:20:10 using *N*-methyl pyrrolidione as a dispersant. The paste was casted onto Al foil and dried at 100°C in the vacuum oven overnight. The 2032 coin cells were assembled for measurement of electrochemical performance with the prepared cathode electrode, Li foil as the counter and reference electrode, 1 M $LiPF_6$ dissolved in ethylene carbonate (EC)/diethyl carbonate (DEC) (1:1 in volume) as electrolyte and polypropylene 2400 as a separator. The cells were galvanostatically charged and discharged using a battery cycler in the voltage range of 3.0-4.3 V (1 C = 133 mAh/g). Electrochemical impedance measurement (EIS) was collected after the 20th charge-discharge cycle in the frequency range from 100 kHz to 10 mHz with an amplitude of 5 mV. All of the electrochemical measurement was carried out at room temperature.

3. Result and discussion

The XRD patterns of the pristine LVP and LVP/graphene composite were shown in Fig. 1. All reflections can be indexed to a well-defined monoclinic space group $P2_1/n$. The peak at approximately 22° in LVP indicated the Li_3PO_4 impurity phase (denoted by a star) due to possible loss of vanadium during the heat treatment [23]. However, no impurity peak was

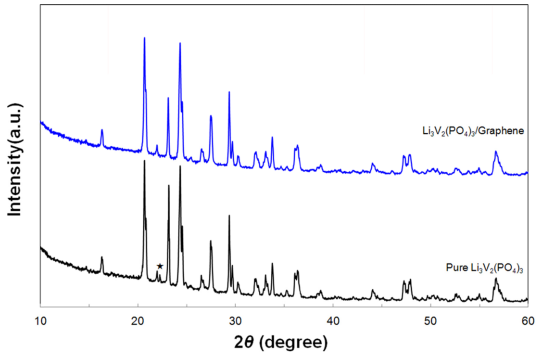

Fig. 1. XRD patterns of the pristine LVP and LVP/graphene composite.

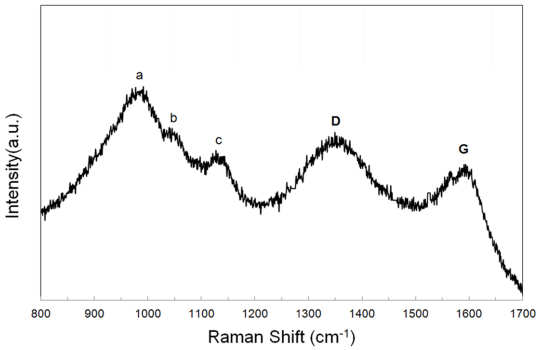

Fig. 2. The Raman spectrum of the LVP/graphene.

observed in the LVP/graphene samples, demonstrating that addition of graphene did not influence the structure and gave the high crystallinity of the LVP. It is also indicating that the intense reflection peaks showed the high quality of the sample. There was no peak related to the carbon in XRD pattern, implying the carbon was coated in the amorphous phase. The presence of carbon contents in LVP/grpahene was observed by a Raman spectroscopy and had shown in Fig. 2. As can be seen, there are two broad peaks at 1345 cm^{-1} and 1585 cm^{-1} which are corresponding to the D-band (disorder induced phonon mode) and G-band (E_{2g} vibration of graphite) of carbon, respectively [24]. The presence of D-band and G-band is suggesting that the graphene plays a role of improving the electronic conductivity and electrochemical performance [25-26]. In addition, the peaks denoted by a, b and c in Fig. 2 indicated the vibration of $Li_3V_2(PO_4)_3$ [27,28].

Fig. 3 shows the SEM images of the pristine LVP and LVP/graphene composite. The LVP had larger particle size than that of LVP/graphene and severely agglomerated particles as shown in Fig. 3a. However, when the graphene was added in the LVP, the morphology of the LVP/graphene sample showed the well-crystallized and smaller particles with some clusters. The LVP/graphene composites were enwrapped into the graphene nanosheets and also strongly adhered to the surface of the graphene layer. It is indicating that the addition of graphene has notable effect on the morphology and particle size during the sintering. It is also believed to that the fine particle size can affect the improved electrochemical performance due to large surface area [25,29]. After addition of the graphene, the particles are well-connected with each other in the LVP/graphene particles.

In order to evaluate effect of the graphene addition in the LVP/graphene composite, electrochemical performance test was conducted. Fig. 4a shows the first charge-discharge curves of the LVP and LVP/graphene composite in the potential range of 3.0-4.3 V at 0.1 C. As shown in Fig. 4a, all the composites showed obviously three charge and discharge plateaus, which are identified as the two-phase transition processes during electrochemical reactions [6-9,30]. The first oxidation peaks around 3.6 and 3.7 V correspond to the removal of first Li in two steps, since there is an ordered $Li_{2.5}V_2(PO_4)_3$ phase. Another Li is extracted at around 4.1 V corresponding to the oxidation of V^{3+} to V^{4+}. The three reduction

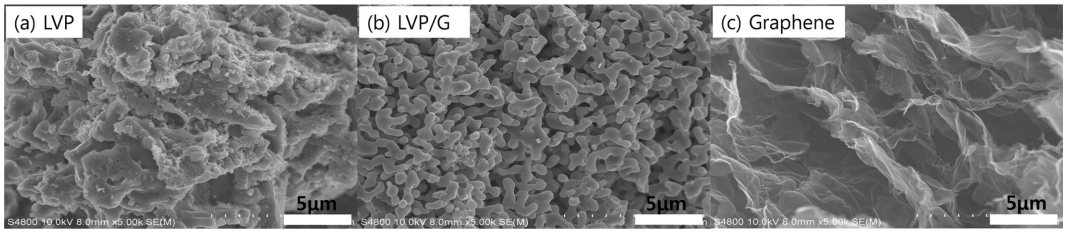

Fig. 3. The SEM images of (a) the pristine LVP, (b) LVP/grpahene and (c) graphene.

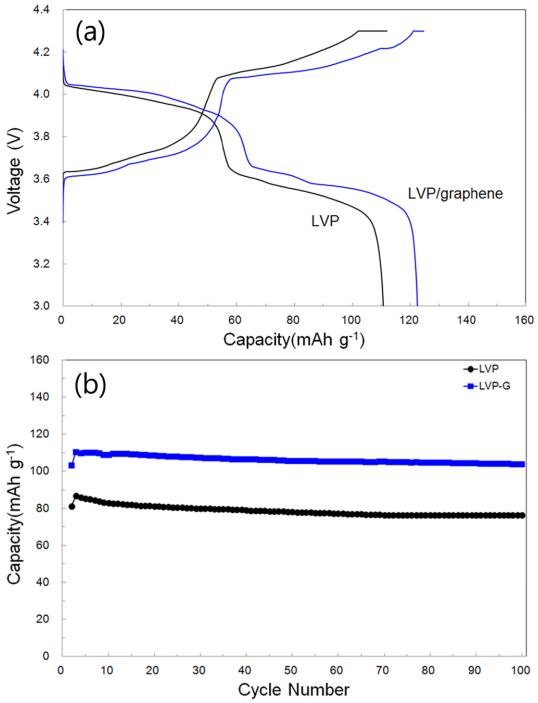

Fig. 4. (a) The initial charge-discharge voltage profile of the pristine LVP and LVP/graphene at 0.1 C and (b) the cycling performance at 0.5 C.

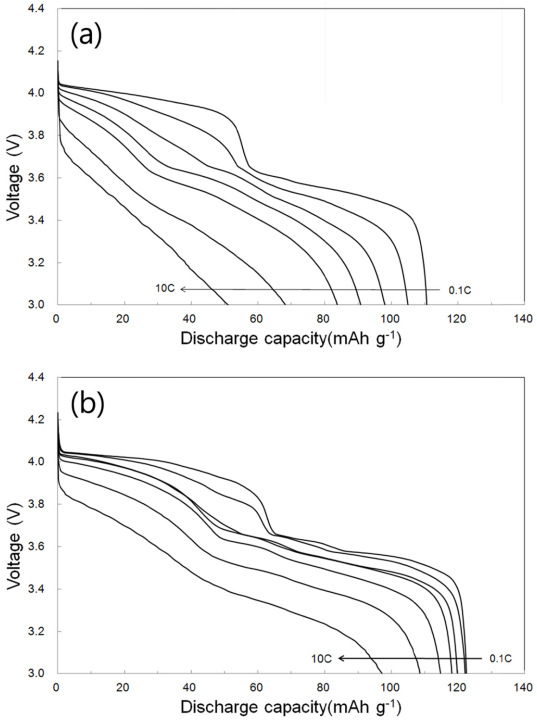

Fig. 5. The rate capability of (a) the pristine LVP and (b) LVP/graphene composites at 0.1, 0.2, 0.5, 1, 2, 5 and 10 C.

peaks was also observed at 3.9, 3.6 and 3.5 V corresponding to the reinsertion of the two Li^+ ions, associated with V^{4+}/V^{3+} redox couple [31,32]. The capacity of LVP/graphene electrode was calculated based on active material including carbon content. Graphene content was about 2 wt%. The LVP/graphene electrode exhibited the initial charge capacity of 125 mAh g^{-1} at 0.1 C and a subsequent discharge capacity of 122 mAh g^{-1} with a Coulombic efficiency of ~98%. In comparison, the pristine LVP delivered a discharge capacity of 111 mAh g^{-1} and Coulombic efficiency (~88%). The LVP/graphene showed the larger charge and discharge capacity and smaller potential differences of the plateaus compared with pristine LVP sample. It is indicating that the composite has a lower electrochemical polarization and leads to the better reversibility in the charge-discharge processes. In addition, the LVP/graphene electrode exhibited the higher discharge capacity and very stable capacity retention during 100cycles as shown in Fig. 4b. The LVP/graphene delivered the discharge capacity of 105 mAh g^{-1} after 100cycles much higher than the pristine LVP (76 mAh g^{-1}). The capacity retention ratio of the LVP/graphene and pristine LVP was 94.0 % and 88.4% after 100cycles, respectively. Therefore, the LVP/graphene composites have higher discharge capacity and better cycle ability. A high C-rate performance is important factor to make the high power/fast Li ion batteries. Fig. 5 shows the rate capability of both LVP and LVP/graphene samples. The pristine LVP electrode showed poor rate capability, giving the discharge capacity of 114, 105, 98, 91, 83, 67 and 50 mAh g^{-1} at current density of 0.1, 0.2, 0.5, 1, 2, 5 and 10 C, respectively. The poor rate capability of the LVP electrode is mainly attributed to their low electrical conductivity. However, the LVP/graphene electrode showed the high discharge capacities of 123, 122, 120, 118, 115, 109 and 98 mAh g^{-1} at current rates of 0.1, 0.2, 0.5, 1, 2, 5 and 10 C, respectively. It can be seen that the rate capability of the LVP/graphene was significantly improved compared with that of the pristine LVP. The improved rate capability of the LVP/graphene electrode is due to the highly conductive graphene nano-powder resulting in enhancing the charge transfer in the electrode. Furthermore, the primary particles are well-connected each other and

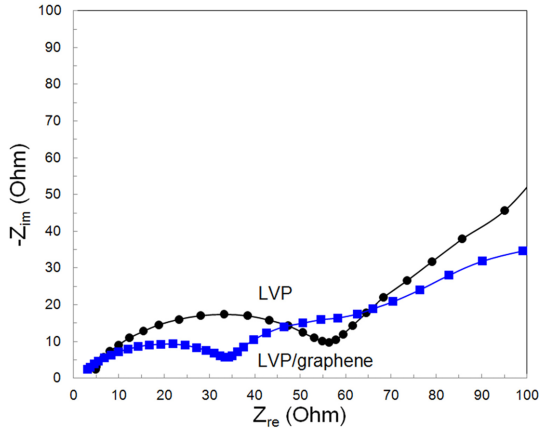

Fig. 6. The electrochemical impedance spectroscopy of the pristine LVP and LVP/graphene.

shorten the diffusion distance for Li ion intercalation/de-intercalation reaction. In order to investigate the electrode reaction kinetics of the samples, the EIS measurements were carried out for the pristine LVP and LVP/graphene electrodes. Fig. 6 shows the EIS spectra of both samples after the 20th cycles. Both electrodes exhibited a semicircle in the high-frequency range and an inclined line in the low-frequency range. The high-frequency range semicircle is assigned to the charge-transfer impedance in the electrode/electrolyte, and the inclined line corresponds to the lithium-ion diffusion process [33-35]. The charge-transfer impedance for the pristine LVP and LVP/graphene electrodes are 54.9 and 32.3 Ω, respectively, indicating that the presence of the graphene significantly decreased the charge-transfer of the LVP/graphene electrode. And also, the improved electrical conductivity led to the enhanced rate capabilities of LVP/graphene composite. Moreover, the graphene influenced the morphology of the LVP electrode, giving the good network for low conductance of the pristine LVP sample. As a result, the electrochemical performance of the LVP/graphene sample was improved. In addition, there is only one semicircle in both samples in the high-frequency range even after the 20th cycles. It means no SEI formation on the cathode surface of both samples at least 20th cycles. The SEI films typically decreased the electronic conductivity by forming a gel-like polymer containing LiF, Li_2CO_3 and lithium alkyl carbonate ($ROCO_2Li$).[34,36] It could be concluded that the introduction of graphene can stabilize the LVP surface and prohibit the side-reaction during the charging-discharging process.

4. Conclusion

In summary, the LVP/graphene composite has been simply prepared by adding the graphene nano-powder. The addition of graphene reduced the impurity of the LVP and showed the fine particle size which could enhance the electrical conductivity. Compared with the pristine LVP, LVP/graphene exhibited the higher dis charge capacity and the rate capability. The LVP/graphene composite showed the discharge capacity of 98 mAh g^{-1} at 10 C in the potential range of 3.0-4.3 V and the capacity retention ration is 94.0% after 100cycles. Due to the fine particles and morphology of the LVP/graphene composites, the electrical conductivity was improved in EIS measurement, indicating that the LVP/graphene composite makes it practical as the cathode materials for LIBs.

Acknowledgements

This work was supported by the Industrial Strategic Technology Development Program (10045401, Development of high-voltage multi-transition metal phosphate cathode material) funded by the Ministry of Trade, Industry & Energy(MOTIE, Korea).

References

[1] B. Kang and G. Ceder, *Nature*, **458**, 190 (2009).
[2] X. Wang, X. Cao, L. Bourgeois, H. Guan, S. Chen, Y. Zhong, D. M. Tang, H. Li, T. Zhai and L. Li, *Adv. Funct. Mater.*, **22**, 2682 (2012).
[3] H. Song, K. T. Lee, M. G. Kim, L. F. Nazar and J. Cho, *Adv. Funct.Mater.*, **20**, 3818 (2010).
[4] J. Gopalakrishnan, *K.K. Rangan, Chem. Mater.* **4**, 745, (1992).
[5] M.Y. Saidi, J. Barker, H. Huang, J.L. Swoyer, and G. Adamson, *Electrochem. Solid State Lett*. **5**, A149 (2002).
[6] S.C. Yin, H. Grondey, P. Strobel, M. Anne, L.F. Nazar, and J. Am. *Chem. Soc*. **125**, 10402 (2003).
[7] S.C. Yin, H. Grondey, P. Strobel, H. Huang, L.F. Nazar, and J. Am. *Chem. Soc*. **125**, 326 (2003).
[8] H. Huang, S.C. Yin, T. Kerr, N. Taylor, and L.F. Nazar, *Adv. Mater*. **14**, 1525 (2002).
[9] M.Y. Saidi, J. Barker, H. Huang, J.L. Swoyer, and G. Adamson, *J. Power Sources* **266**, 119 (2003).
[10] X. Rui, N. Ding, J. Liu, C. Li, and C. Chen, *Electrochim. Acta*, **55**, 2384 (2010).
[11] A. Pan, J. Liu, J. G. Zhang, W. Xu, G. Cao, Z. Nie, B. W. Arey, and S. Liang, *Electrochem. Commun.*, **12**, 1674 (2010).
[12] P. Fu, Y. Zhao, Y. Dong, X. An, and G. Shen, *J. Power*

Sources, **162**, 651 (2006).
[13] Q. Chen, X. Qiao, Y. Wang, T. Zhang, C. Peng, W. Yin, and L. Liu, *J. Power Sources*, **201**, 267 (2012).
[14] Y. Chen, Y. Zhao, X. An, J. Liu, Y. Dong, and L. Chen, *Electrochim. Acta*, **54**, 5844 (2009).
[15] C. Dai, Z. Chen, H. Jin, and X. Hu, *J. Power Sources*, **195**, 5775 (2010).
[16] M. Bini, S. Ferrari, D. Capsoni, and V. Massarotti, *Electrochim. Acta*, **56**, 2648 (2011).
[17] C. Sun, S. Rajasekhara, Y. Dong, and J. B. Goodenough, *ACS Appl. Mater. Interfaces*, **3**, 3772 (2011).
[18] X. Du, W. He, X. Zhang, Y. Yue, H. Liu, D. Min, X. Ge, and Y. Du, *J. Mater. Chem*., **22**, 5960 (2012).
[19] C. Chang, J. Xiang, X. Shi, X. Han, L. Yuan, and J. Sun, *Electrochim. Acta*, **54**, 623 (2008).
[20] L. Wang, L. C. Zhang, I. Lieberwirth, H. W. Xu, and C. H. Chen, *Electrochem. Commun.*, **12**, 52 (2010).
[21] Y. Qiao, X. Wang, J. Xiang, D. Zhang, W. Liu, and J. Tu, *Electrochim. Acta*, **56**, 2269 (2011).
[22] H. Liu, P. Gao, J. Fang, and G. Yang, *Chem. Commun*., **47**, 9110 (2011).
[23] L. Fei, W. Lu, Li Sun, J. Wang, J. Wei, H.L.W. Chan, and Y. Wang, *RSC Adv.*, **3**, 1297 (2013).
[24] A. Ferrari and J. Robertson, *Phys. Rev. B: Condens. Matter*, **61**, 14095 (2000).
[25] J.W. Wang, J. Liu, G.L. Yang, X.F. Zhang, X.D. Yan, X.M. Pan, and R.S. Wang, *Electrochim. Acta*, **54**, 6451 (2009).
[26] Y.Q. Qiao, J.P. Tu, X.L. Wang, D. Zhang, J.Y. Xiang, Y.J. Mai, and C.D. Gu, *J. Power Sources*, **196**, 7715 (2011).
[27] C.M. Burba and R. Frech, *Solid State Ionics*, **177**, 3445 (2007).
[28] J.S. Huang, L. Yang, K.Y. Liu, and Y.F. Tang, *J. Power Sources*, **195**, 5013 (2010).
[29] L. Wang, G.C. Liang, X.Q. Ou, X.K. Zhi, J.P. Zhang, and J.Y. Cui, *J. Power Sources*, **189**, 423 (2009).
[30] M.Y. Saidi, J. Barker, H. Huang, J.L. Swoyer, and G. Adamson, *Electrochem. Solid State Lett.* **5**, A149 (2002).
[31] X. Zhu, Y. Liu, L. Geng, and L. Chen, *J. Power Sources*, **184**, 578 (2008).
[32] L. Wang, X. Zhou, and Y. Guo, *J. Power Sources*, **195**, 2844 (2010).
[33] X.H. Huang, J.P. Tu, C.Q. Zhang, X.T. Chen, Y.F. Yuan, and H.M. Wu, *Electrochim. Acta,* **52**, 4177 (2007).
[34] M. Takahashi, S.-I. Tobishima, K. Takei, and Y. Sakurai, *Solid State Ionics*, **148**, 283, (2002).
[35] S.B. Yang, H.H. Song, and X.H. Chen, *Electrochem. Commun*., **8**, 137 (2006).
[36] S. Grugeon, S. Laruelle, R. Herrera-Urbina, L. Dupont, P. Poziot, J.M. Tarascon, J. Electrochem. Soc., **148**, A285 (2001).